Acta Crystallographica Section D
Biological Crystallography
ISSN 0907-4449

Inhibitory properties and X-ray crystallographic study of the binding of AR-101, AR-102 and iclaprim in ternary complexes with NADPH and dihydrofolate reductase from *Staphylococcus aureus*

Christian Oefner,‡ Sandro Parisi, Henk Schulz,§ Sergio Lociuro and Glenn E. Dale*

Arpida Ltd, CH-4153 Reinach, Switzerland

‡ Present address: Polyphor Ltd, Allschwil, Switzerland.
§ Present address: Novartis AG, Basel, Switzerland.

Correspondence e-mail: glenn.dale@arpida.com

Received 28 January 2009
Accepted 14 April 2009

PDB References: DHFR–iclaprim complexes, 3fy8, r3fy8sf; 3fy9, r3fy9sf; 3fyv, r3fyvsf; 3fyw, r3fywsf.

Iclaprim is a novel dihydrofolate reductase (DHFR) inhibitor belonging to the 2,4-diaminopyrimidine class of antibiotics, of which trimethoprim (TMP) is the most well known representative. Iclaprim exhibits potent bactericidal activity against major Gram-positive pathogens, notably methicillin-sensitive *Staphylococcus aureus* (MSSA) and methicillin-resistant *S. aureus* (MRSA) phenotypes, including TMP-resistant strains. The inhibition properties of racemic iclaprim and of the two enantiomers, termed AR-101 and AR-102, towards *S. aureus* wild-type DHFR and TMP-resistant F98Y mutant DHFR were determined and compared. Similar to TMP, AR-101, AR-102 and iclaprim are all competitive inhibitors with respect to the substrate dihydrofolate. Iclaprim, AR-101 and AR-102 demonstrated little or no difference in activity towards these enzymes and were significantly more potent than TMP. The crystal structures of *S. aureus* DHFR and F98Y mutant DHFR were determined as ternary complexes with NADPH and either AR-101, AR-102 or iclaprim. The binding modes of the inhibitors were analysed and compared. The X-ray crystallographic data explain the binding modes of all molecules well and can be used to rationalize the equipotent affinity of AR-101, AR-102 and iclaprim, which is also reflected in their antibacterial properties.

1. Introduction

DHFR (EC 1.5.1.3) catalyzes the transfer of a hydride ion from nicotinamide adenine dinucleotide phosphate (NADPH) to 7,8-dihydrofolate (DHF), forming the product 5,6,7,8-tetrahydrofolate (THF). DHFR is a key enzyme in the THF pathway as it is essential for maintaining the intracellular pools of THF and its derivatives, which are essential cofactors in a number of one-carbon transfer reactions, including those involved in the biosynthesis of thymidylate, methionine, purine nucleotides, panthothenate and other metabolites (Kompis *et al.*, 2005). Inhibition of this enzyme arrests DNA synthesis and cell division, leading to cell death. Owing to this important role, chromosomal DHFRs have been the target of small-molecule therapeutics in the treatment of cancer as well as bacterial and parasitic infections (Then, 2004; Kompis *et al.*, 2005; Hawser *et al.*, 2006). As a consequence of its importance, a wealth of information has been generated on the structure, mechanism and inhibition of DHFR from human, parasitic, fungal and bacterial sources (Schnell *et al.*, 2004).

Trimethoprim (TMP) is a clinically important inhibitor of bacterial DHFRs. TMP has been described as a competitive

inhibitor of dihydrofolate reductase with a greatly increased potency towards the bacterial enzymes (Stone & Morrison, 1986). Owing to this selectivity over human DHFR, TMP has been widely used clinically as a treatment for community-acquired infections, particularly of the urinary and respiratory tract, with emphasis on Gram-negative pathogens. TMP is frequently used in combination with sulfamethoxazole (SMX) and the synergistic activity of these folate-synthesis inhibitors not only results in increased antibacterial activity but also in a decreased propensity for the development of resistance. More recently, TMP/SMX has found use in the treatment of community-acquired methicillin-resistant *Staphylococcus aureus* infections (CA-MRSA; Adra & Lawrence, 2004; Grim *et al.*, 2005; Markowitz *et al.*, 1992; Turnidge & Grayson, 1993). A point mutation in *S. aureus* DHFR (Phe98Tyr) has been shown to lead to resistance to TMP, although epidemiologically the resistance rate is low (1–5%). The point mutation results in the loss of a hydrogen bond and a decreased affinity of TMP for the mutated enzyme. Consequently, DHFR inhibitors with increased potency could be expected to overcome this resistance mechanism and could additionally circumvent the use of the combination with SMX and thus avoid the undesirable side-effects associated with SMX.

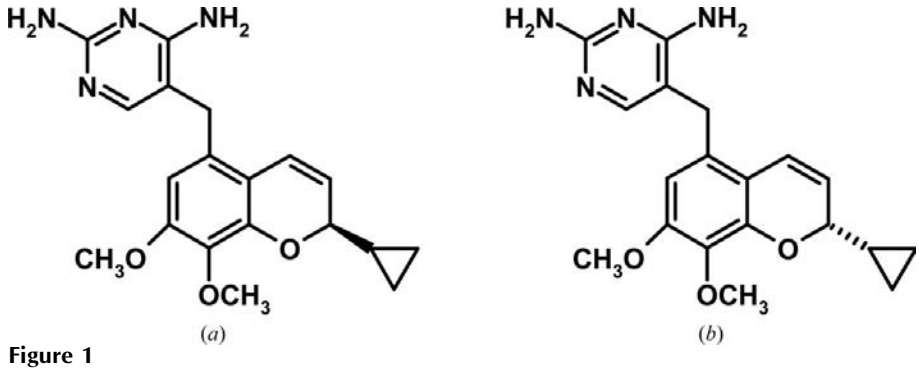

Figure 1
Chemical structures of AR-101 (*a*) and AR-102 (*b*).

Iclaprim {5-[(2-*R,S*)-2-cyclopropyl-7,8-dimethoxy-2*H*-chromene-5-ylmethyl]pyrimidine-2,4-diamine; formerly AR-100} is a novel 2,4-diaminopyrimidine that exhibits potent rapidly bactericidal activity against major Gram-positive pathogens, most notably the MSSA and MRSA phenotypes, including TMP-resistant strains, and β-haemolytic streptococci including *Streptococcus pyogenes* and *Strep. agalactiae*. Moreover, iclaprim demonstrates a good distribution in tissues and organs and is safe and well tolerated. Iclaprim specifically and selectively inhibits bacterial DHFR at submicromolar concentrations, with no inhibition of the human enzyme at concentrations that are over four orders of magnitude higher (Schneider *et al.*, 2003). Understanding the mechanism of resistance to TMP led to the design of this new inhibitor with improved affinity towards *S. aureus* DHFR. A detailed comparison of the modes of action of iclaprim and TMP towards *S. aureus* has recently been described (Oefner *et al.*, 2009). Iclaprim maintains a clinically useful activity towards *S. aureus*, including those resistant to TMP. At present, Arpida AG (http://www.arpida.ch) has completed two Phase III clinical trials for intravenous iclaprim for its first indication: complicated skin and skin-structure infections (cSSSI). Iclaprim, however, is produced and administered as a racemic mixture of two enantiomers: 5-[(2-*R*)-2-cyclopropyl-7,8-dimethoxy-2*H*-chromene-5-ylmethyl]pyrimidine-2,4-diamine (AR-101) and 5-[(2-*S*)-2-cyclopropyl-7,8-dimethoxy-2*H*-chromene-5-ylmethyl]pyrimidine-2,4-diamine (AR-102). The purpose of this study was to characterize the binding properties of the single enantiomers AR-101 and AR-102 by X-ray crystallography and to compare them with iclaprim (Fig. 1).

2. Materials and methods

2.1. Reagents

TMP was purchased from Fluka (catalogue No. F92131). Iclaprim was produced at AMCIS (AMCIS L991001, Switzerland). AR-101 and AR-102 were kindly provided by Dr Peter Schneider (Arpida AG). Reduced nicotinamide adenine diphosphate (NADPH) and 7,8-dihydrofolate were purchased from Fluka (Fluka Chemicals, Switzerland). The purification of wild-type *S. aureus* DHFR and TMP-resistant *S. aureus* F98Y mutant DHFR have been described previously (Dale *et al.*, 1997).

2.2. Enzymatic assay

The *in vitro* DHFR assay was performed essentially as described previously (Baccanari & Joyner, 1981). DHFR activities were determined using a PowerWave HT spectrophotometer. All reactions were performed in a 1 ml reaction volume using a 1 ml Bio-cell with 50 m*M* Tris–HCl pH 7.5, 50 m*M* NaCl, 1 m*M* EDTA, 10 m*M* β-mercaptoethanol, 50 μM DHF, 100 μM NADPH and an appropriate amount of bacterial DHFR enzyme. The oxidation of NADPH by DHFR was monitored by following the change in absorbance at 340 nm. The reaction was initiated by the addition of DHF. The concentration of DHF was measured spectrophotometrically at 282 nm using a molar extinction coefficient of $2.8 \times 10^4\ M^{-1}\ cm^{-1}$ at pH 7.4 (Blakley, 1960). The concentration of NADPH was determined spectrophotometrically at 340 nm using a molar extinction coefficient of $6.2 \times 10^4\ M^{-1}\ cm^{-1}$ (Appleman *et al.*, 1992). The IC_{50} was defined as the concentration of drug required to inhibit 50% of the enzymatic activity. Kinetic parameters were determined by titrating inhibitor (0, 0.75, 1.5, 2.5 and 5 n*M*) and substrate concentrations (3.12, 6.25, 12.5, 25, 50 and 100 μM) in the DHFR enzyme assay. Inhibition constants (K_i) were calculated from Dixon plots [reciprocal of the velocity ($1/v$) against the concentration of inhibitor (I); Dixon, 1953]. The mode of inhibition was determined by plotting the substrate (a)/v

against the concentration of inhibitor (*i*) (Cornish-Bowden, 1974).

2.3. Crystallization, data collection and refinement

Crystals of both wild-type and TMP-resistant F98Y single-mutant DHFR from *S. aureus* were obtained at 297 K using the hanging-drop vapour-diffusion technique. Prior to crystallization, 5 m*M* NADPH and 0.3 mg ml^{-1} inhibitor were added to the concentrated protein solutions (∼30 mg ml^{-1}). Hexagonal bipyramids grew in 25% PEG 3350, 200 m*M* NaCl and 100 m*M* bis-tris pH 5.5. The crystals belonged to the hexagonal space group $P6_122$ and contained one molecule in the asymmetric unit. Prior to data collection, crystals were flash-frozen at 100 K. Diffraction intensities were measured with Cu $K\alpha$ radiation obtained from a Nonius FR591 rotating-anode generator equipped with an Osmic mirror system and were recorded on a MAR Research image-plate area detector. All diffraction data were processed and scaled with *DENZO* and *SCALEPACK* (Otwinowski, 1993) and analyzed further using the *CCP*4 program suite (Collaborative Computational Project, Number 4, 1994). The structure was solved by molecular replacement using the coordinates of *S. aureus* DHFR complexed with folate (Dale *et al.*, 1997) as a model. Density fitting was performed with the graphics program *MOLOC* (Gerber, 1992) and *REFMAC* (Murshudov *et al.*, 1997) was used for stereochemically restrained positional and temperature-factor refinement, using parameters for ideal stereochemistry as described by Engh & Huber (1991). The initial difference densities indicated the presence of the inhibitors; however, all protein structures were initially refined in the absence of the ligand in order to eliminate bias in the electron density. Crystallographic data and refinement statistics are summarized in Table 2.

3. Results and discussion

The kinetic properties of iclaprim, AR-101 and AR-102 were compared against *S. aureus* wild-type chromosomal DHFR and TMP-resistant single-mutant F98Y DHFR (Dale *et al.*, 1997). Similar to TMP and iclaprim, AR-101 and AR-102 exhibited a competitive mode of inhibition towards the *S. aureus* wild-type and F98Y enzymes (Oefner *et al.*, 2009). As shown in Table 1, iclaprim, AR-101 and AR-102 all showed a similar K_i for inhibition of the wild-type DHFR and were all about an order of magnitude more potent than TMP. Similarly, these compounds showed

Table 1
Enzyme-inhibition data for wild-type and resistant *S. aureus* DHFR.

	K_i iclaprim (n*M*)	K_i AR-101 (n*M*)	K_i AR-102 (n*M*)	K_i TMP (n*M*)
WT	0.2 ± 0.07	0. 23 ± 0.15	0.22 ± 0.07	6 ± 0.9
F98Y	2.6 ± 0.57	0.9 ± 0.14	3.5 ± 1.2	100 ± 13

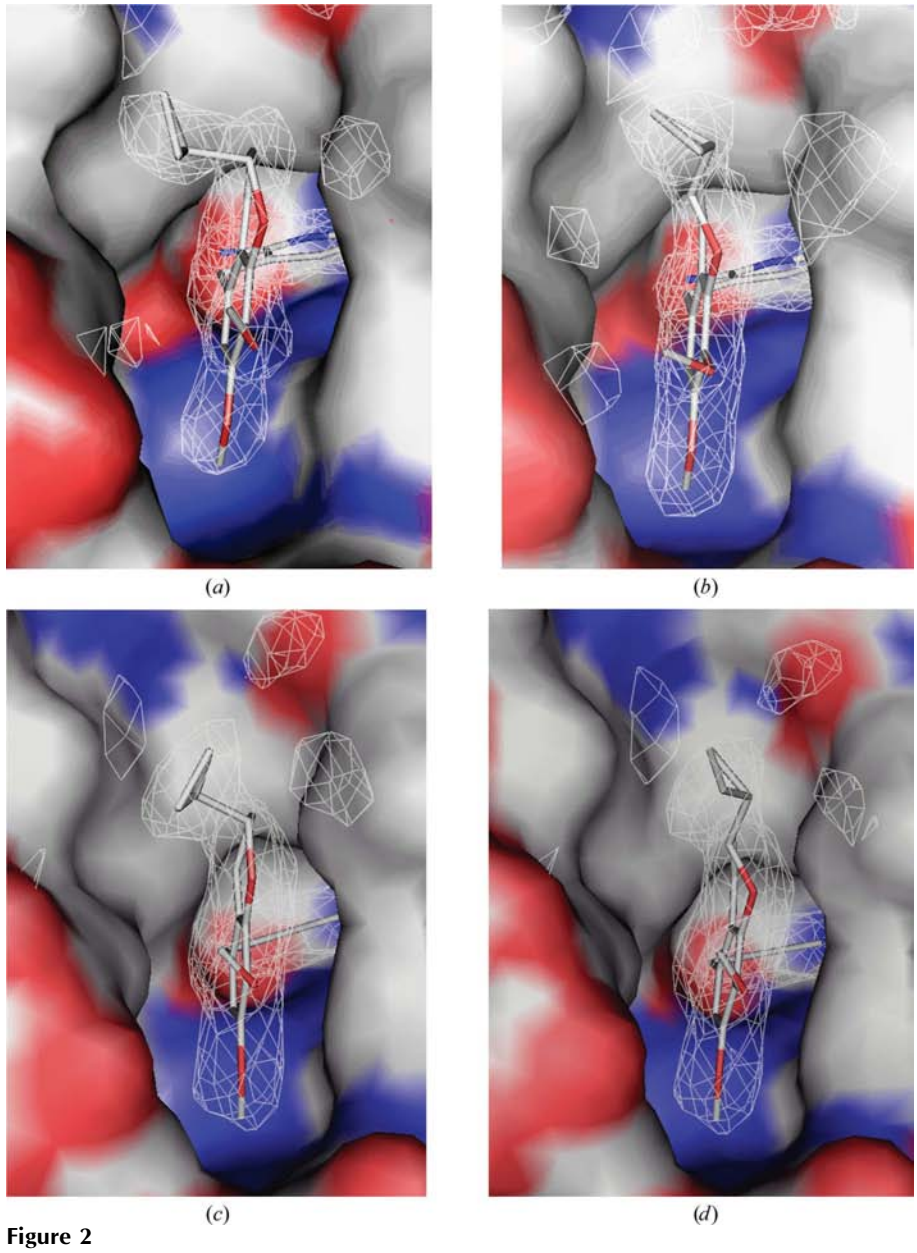

Figure 2
Inhibitor binding to the TMP-resistant F98Y single-mutant dihydrofolate reductase from *S. aureus*. The final $2F_o - F_c$ difference electron density contoured at 1.5σ is shown as white mesh and is superimposed with the structures of AR-101 (*a*), AR-102 (*b*), iclaprim/AR-101 (*c*) and iclaprim/AR-102 (*d*) as observed in ternary complexes with NADPH. The molecular surface of the active site is indicated and coloured by electrostatic potential: blue, positive; red, negative. Unoccupied density corresponds to water molecules. This figure was generated using *PyMOL* (DeLano, 2002).

Table 2
Data-collection and refinement statistics.

Values in parentheses are for the outer shell. Iclaprim is a racemic mixture of AR-101 and AR-102.

	F98Y NADPH Iclaprim	F98Y NADPH AR-101	F98Y NADPH AR-102	Wild type NADPH Iclaprim	Wild type NADPH AR-101	Wild type NADPH AR-102
Crystallographic data						
Unit-cell parameters						
$a = b$ (Å)	79.3	79.6	79.4	79.0	79.1	79.1
c (Å)	108.1	109.0	108.6	107.8	108.4	107.8
Resolution range (Å)	20.0–2.50 (2.66–2.50)	20.0–2.20 (2.34–2.20)	20.0–2.25 (2.39–2.25)	20.0–2.10 (2.23–2.10)	20.0–2.10 (2.44–2.30)	20.0–2.20 (2.34–2.20)
No. of observed reflections	33276	90924	41688	63114	68178	83028
No. of unique reflections	7097	10269	9334	11867	11812	10357
$R_{\rm merge}$† (%)	13.9 (65.4)	16.7 (57.4)	18.1 (88.7)	8.2 (55.8)	8.9 (71.6)	13.8 (75.4)
$I/\sigma(I)$	10.6 (1.7)	14.5 (4.1)	8.3 (1.6)	18.7 (1.8)	19.3 (1.5)	18.6 (1.8)
Completeness (%)	95.5 (87.8)	93.8 (71.0)	91.6 (82.5)	97.5 (85.4)	96.2 (77.6)	97.3 (83.9)
Refinement statistics						
Resolution range (Å)	20–2.50	20–2.20	20–2.25	20–2.10	20–2.10	20–2.20
$R_{\rm cryst}$‡ (%)	21.2	25.1	21.9	21.8	21.9	22.1
$R_{\rm free}$‡ (%)	30.7	33.5	30.2	26.8	26.3	28.9
No. of protein atoms	1283	1273	1273	1282	1282	1282
No. of water molecules	63	157	158	106	125	91
No. of ligand atoms	26	26	26	26	26	26
No. of NADPH atoms	48	48	48	48	48	48
Mean B factors (Å^2)						
Protein atoms	42.8	20.5	40.1	42.8	43.9	45.5
Ligand atoms	R 47.8, S 45.4	18.4	38.3	R 59.1, S 59.7	50.4	55.4
NADPH atoms	43.1	16.2	37.1	42.3	43.8	46.3
R.m.s.d.§ bonds (Å)	0.01	0.011	0.009	0.006	0.004	0.007
R.m.s.d.§ angles (°)	1.70	1.59	1.21	1.34	0.82	1.09

† $R_{\rm merge} = \sum_{hkl}\sum_i |I_i(hkl) - \langle I(hkl)\rangle| / \sum_{hkl}\sum_i I_i(hkl)$, where $I_i(hkl)$ and $\langle I(hkl)\rangle$ are the ith and the mean measurement of the intensity of reflection hkl. ‡ $\sum_{hkl} ||F_{\rm obs}| - |F_{\rm calc}|| / \sum_{hkl} |F_{\rm obs}|$, where $|F_{\rm obs}|$ and $|F_{\rm calc}|$ are the observed and calculated structure-factor amplitudes for reflection hkl applied to the working ($R_{\rm cryst}$) and test ($R_{\rm free}$) sets, respectively. § R.m.s.d.: root-mean-square deviation from mean.

potent inhibition of the F98Y mutant DHFR which was at least one order of magnitude better than TMP and similar to the $K_{\rm i}$ of TMP against the wild-type enzyme. The small differences observed between iclaprim, AR-101 and AR-102 are most likely to reflect the difficulty in the determination of the true $K_{\rm i}$ owing to the fact that the $K_{\rm i}$ values approach the concentration of the enzyme used in the assay (Copeland *et al.*, 1995).

The binding of the compounds AR-101 (Fig. 1*a*) and AR-102 (Fig. 1*b*) as well as the binding of iclaprim to the TMP-resistant F98Y single-mutant DHFR from *S. aureus* and the TMP-sensitive wild-type enzyme has been determined in ternary complexes with NADPH by X-ray crystallography using cocrystallization experiments. Refinement of the structural data obtained for the ternary complexes of AR-101, AR-102 and iclaprim with the TMP-resistant F98Y single-mutant enzyme in the presence of NADPH converged to R factors of 0.251, 0.219 and 0.212 in the resolution ranges 20.0–2.20, 20.0–2.25 and 20.0–2.50 Å, respectively (Table 2). Figs. 2(*a*) and 2(*b*) show the final $2F_{\rm o} - F_{\rm c}$ difference electron densities for AR-101 and AR-102 calculated with phases from the refined structures. The binding of AR-101 and AR-102 is clearly defined in the mutant enzyme; the mean isotropic temperature factors of the two ligands are 18.4 and 38.3 Å^2, respectively, and correspond to those observed for all protein atoms of 20.5 and 40.1 Å^2, respectively. The experimental data obtained for the ternary complex with iclaprim revealed the binding of both stereoisomers, AR-101 and AR-102, as verified by their independent structural refinement, which led to similar mean temperature factors for the R and S conformers of 47.8 and 45.4 Å^2 compared with 42.8 Å^2 for all atoms of the protein. The final $2F_{\rm o} - F_{\rm c}$ difference electron densities of iclaprim calculated with phases from the independently refined structure of AR-101 or AR-102 are shown in Figs. 2(*c*) and 2(*d*) superimposed with the respective inhibitor.

Refinement of the structural data obtained for the ternary complexes of AR-101, AR-102 and iclaprim with the wild-type enzyme in the presence of NADPH converged to R factors of 0.219, 0.221 and 0.218 in the resolution ranges 20.0–2.10, 20.0–2.20 and 20.0–2.10 Å, respectively (Table 2). Figs. 3(*a*) and 3(*b*) show the final $2F_{\rm o} - F_{\rm c}$ difference electron densities for the respective inhibitors calculated with phases from the refined structures. The final $2F_{\rm o} - F_{\rm c}$ difference electron densities of iclaprim calculated with phases from the independently refined structure of AR-101 or AR-102 are shown in Figs. 3(*c*) and 3(*d*) superimposed with the respective inhibitor. The experimental data revealed that in all ternary complexes with the wild-type enzyme the cyclopropyl moieties of the respective compounds are partially disordered as reflected in the mean isotropic temperature factors for the ligands, which significantly exceed those observed for the protein in their respective structures.

All protein structures were initially refined in the absence of the ligand in order to eliminate bias in the electron density. As

a result, the binding modes of AR-101 and AR-102 are clearly defined in the F98Y enzyme (Figs. 2*a* and 2*b*). For iclaprim, the AR-101 and AR-102 enantiomers could be fitted equally well to the unbiased electron density (Figs. 2*c* and 2*d*), which is consistent with the observation that there is little or no preference for one enantiomer over the other (K_i = 0.9 n*M* for AR-101 *versus* K_i = 3.5 n*M* for AR-102). The concentration of iclaprim used in the cocrystallization experiments was ∼1 m*M*. In the case of the wild-type enzyme the electron density for AR-101 and AR-102 is less well defined compared with that observed for the F98Y mutant enzyme; nevertheless, the molecules could be fitted to the electron density in both cases with little ambiguity. As expected, in the case of iclaprim the cyclopropyl moiety of both enantiomers was poorly defined. This can be explained in part by the fact that both enantiomers of iclaprim have a similar affinity to the target enzyme (K_i = 0.23 n*M* for AR-101 *versus* K_i = 0.22 n*M* for AR-102). Therefore, both enantiomers of iclaprim interact similarly with the enzyme such that each isomer is bound to the active site with approximately 50% occupancy, which results in a weaker electron density for the cyclopropyl moiety.

The binding modes of both AR-101 and AR-102 to the wild-type and mutant enzymes in the presence of NADPH were also compared. Compared with the wild-type enzyme, the hydroxy function of Tyr98 in the TMP-resistant enzyme alters the orientation and location of the diaminopyrimidine ring away from the nicotinamide moiety of NADPH, resulting in a slight (0.5–0.6 Å) 'upwards' movement of the dimethoxychromene substituent for both compounds (Fig. 4). The altered location is a result of the loss of a single hydrogen bond from the diaminopyrimidine moiety to the protein as previously reported (Dale *et al.*, 1997). However, the altered location of the dimethoxychromene moiety in the F98Y enzyme also leads to a decreased contact-surface area for all compounds in the mutant enzyme compared with the wild-type DHFR. This movement would contribute to the decrease in affinity of the inhibitors towards the mutant enzyme. However, the 'upwards' shift brings the cyclopropyl moiety into closer contact with the protein within the hydrophobic channel. This movement of AR-101 and AR-102 in the TMP-resistant mutant enzyme fixes the cyclopropyl substituent of the dimethoxy chromene moiety, resulting in an ordered orientation with clearly defined electron density. Although the cyclopropyl moieties of AR-101 and AR-102 have slightly different contacts within the active site, they both contribute to the binding of the compound to the mutant protein.

The cyclopropyl-dimethoxychromene moiety interacts with the conserved residues (Leu28, Val31, Ile50 and Leu54) forming a hydrophobic pocket in the enzyme which is the

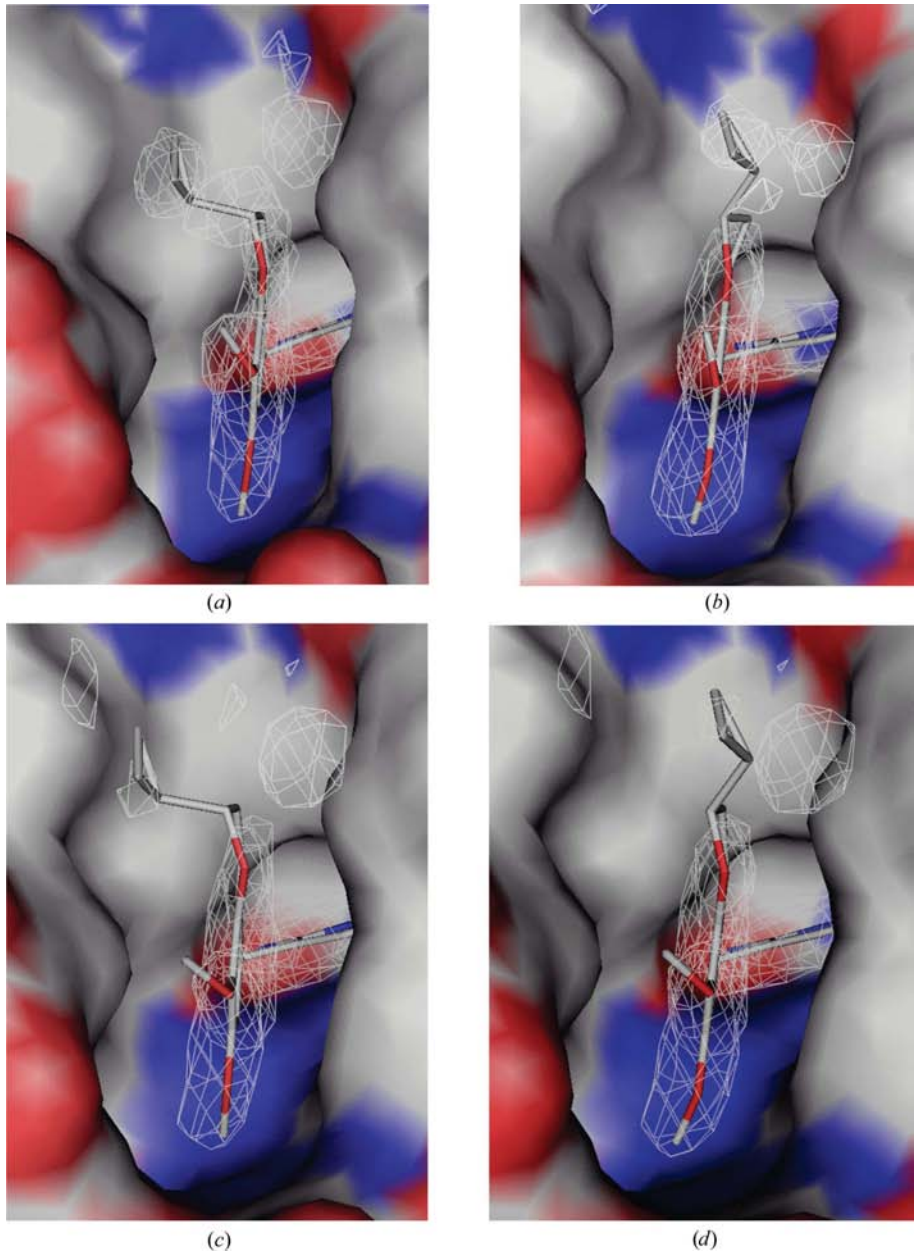

Figure 3
Inhibitor binding to wild-type dihydrofolate reductase from *S. aureus*. The final $2F_o - F_c$ difference electron density contoured at 1.5σ is shown as white mesh and is superimposed with the structures of AR-101 (*a*), AR-102 (*b*), iclaprim/AR-101 (*c*) and iclaprim/AR-102 (*d*) as observed in a ternary complex with NADPH. The molecular surface of the active site is indicated and coloured by electrostatic potential; blue, positive; red, negative. Unoccupied density corresponds to water molecules. This figure was generated using *PyMOL* (DeLano, 2002).

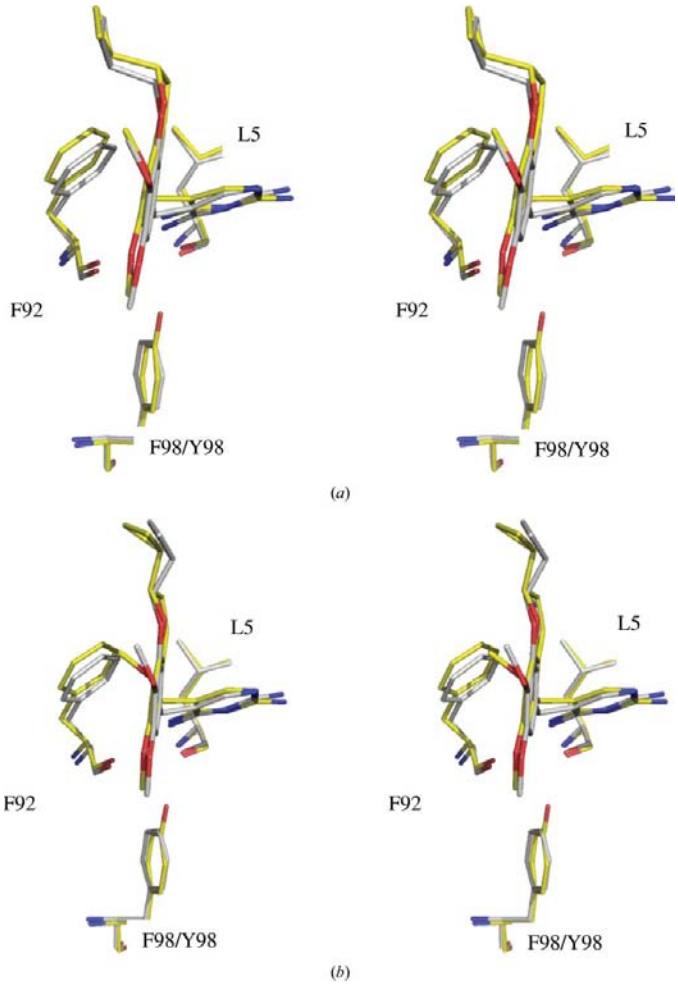

Figure 4
Stereo drawing of the binding of AR-101 (*a*) and AR-102 (*b*) to wild-type (white) and F98Y (yellow) mutant enzyme. The newly introduced hydroxy function of Tyr98 in the TMP-resistant enzyme alters the location of the diaminopyrimidine moiety of the inhibitor by approximately 0.5 Å in both cases. Amino-acid residues are indicated.

binding site for the *p*-aminobenzamide moiety of the substrate dihydrofolate. It is tempting to speculate that the two orientations of the cyclopropyl moiety of iclaprim in the active site would decrease the likelihood of the development of resistance as it interacts mainly with Ile50 and Leu54 in the case of the *R* enantiomer (AR-101) and with Leu28 in the case of the *S* enantiomer (AR-102), which are located on opposite sites of the hydrophobic cavity.

4. Conclusions

Comparison of the kinetic properties of the racemate iclaprim and its enantiomers AR-101 and AR-102 show that all these compounds, like TMP, are competitive inhibitors of DHFR with respect to the substrate dihydrofolate. However, determination of the K_i values show that iclaprim, AR-101 and AR-102 are inhibitors that are one order of magnitude more potent towards both the wild-type and the F98Y mutant DHFR enzymes when compared with TMP. Moreover, the affinity of iclaprim, AR-101 and AR-102 towards the F98Y mutant enzyme is similar to that of TMP towards the wild-type DHFR (Table 1).

The X-ray structures of AR-101, AR-102 and iclaprim have been determined as ternary complexes with NADPH in both wild-type *S. aureus* DHFR and the TMP-resistant F98Y mutant enzyme. In the case of AR-101 and AR-102 the molecules are clearly defined in both the wild-type and F98Y enzyme, while for iclaprim the cyclopropyl moiety is poorly defined. The electron density for the cyclopropyl moiety is decreased by approximately 50% for each orientation, reflecting a decreased occupancy of each enantiomer. This decrease in occupancy can be explained by the comparable affinities of both enantiomers towards the enzyme, leading to equal representation of the *R* and *S* enantiomers in the active site. The experimental data explain the binding modes of all molecules well and can be used to rationalize the increased affinity compared with TMP towards the enzyme as well as the equal affinity of each enantiomer compared with iclaprim, which is also reflected in the antibacterial properties.

We gratefully acknowledge Manon Müller and Marc Meyer for their technical assistance.

References

Adra, M. & Lawrence, K. R. (2004). *Ann. Pharmacother.* **38**, 338–341.
Appleman, J. R., Tsay, J. T., Freisheim, J. H. & Blakley, R. L. (1992). *Biochemistry*, **31**, 3709–3715.
Baccanari, D. P. & Joyner, S. S. (1981). *Biochemistry*, **20**, 1710–1716.
Blakley, R. L. (1960). *Nature (London)*, **188**, 231–232.
Collaborative Computational Project, Number 4 (1994). *Acta Cryst.* D**50**, 760–763.
Copeland, R. A., Lombardo, D., Giannaras, J. & Decicco, C. P. (1995). *Bioorg. Med. Chem. Lett.* **5**, 1947–1952.
Cornish-Bowden, A. (1974). *Biochem. J.* **137**, 143–144.
Dale, G. E., Broger, C., D'Arcy, A., Hartman, P. G., DeHoogt, R., Jolidon, S., Kompis, I., Labhardt, A. M., Langen, H., Locher, H., Page, M. G., Stuber, D., Then, R. L., Wipf, B. & Oefner, C. (1997). *J. Mol. Biol.* **266**, 23–30.
DeLano, W. L. (2002). *The PyMOL User's Manual.* DeLano Scientific, Palo Alto, California, USA.
Dixon, M. (1953). *Biochem. J.* **55**, 170–171.
Engh, R. A. & Huber, R. (1991). *Acta Cryst.* A**47**, 392–400.
Gerber, P. (1992). *Biopolymers*, **32**, 1003–1017.
Grim, S. A., Rapp, R. P., Martin, C. A. & Evans, M. E. (2005). *Pharmacotherapy*, **25**, 253–264.
Hawser, S., Lociuro, S. & Islam, K. (2006). *Biochem. Pharmacol.* **71**, 941–948.
Kompis, I. M., Islam, K. & Then, R. L. (2005). *Chem. Rev.* **105**, 593–620.
Markowitz, N., Quinn, E. L. & Saravolatz, L. D. (1992). *Ann. Intern. Med.* **117**, 390–398.
Murshudov, G. N., Vagin, A. A. & Dodson, E. J. (1997). *Acta Cryst.* D**53**, 240–255.
Oefner, C., Bandera, M., Haldimann, A., Laue, H., Schulz, H., Mukhija, S., Parisi, S., Weiss, L., Lociuro, S. & Dale, G. E. (2009). *J. Antimicrob. Chemother.* **63**, 687–698.
Otwinowski, Z. (1993). *Proceedings of the CCP4 Study Weekend. Data Collection and Processing*, edited by L. Sawyer, N. Isaacs & S. Bailey, pp. 56–62. Warrington: Daresbury Laboratory.

Schneider, P., Hawser, S. & Islam, K. (2003). *Bioorg. Med. Chem. Lett.* **13**, 4217–4221.
Schnell, J. R., Dyson, H. J. & Wright, P. E. (2004). *Annu. Rev. Biophys. Biomol. Struct.* **33**, 119–140.
Stone, S. R. & Morrison, J. F. (1986). *Biochim. Biophys. Acta*, **869**, 275–285.
Then, R. L. (2004). *J. Chemother.* **16**, 3–12.
Turnidge, J. & Grayson, M. L. (1993). *Drugs*, **45**, 353–366.